A new approach for dry metal forming: CO_2 as volatile lubrication in combination with hard and low friction coatings

Georg Umlauf[1,*], *Henning* Hasselbruch[2], *Jan Hinnerk* Henze[1], *Jakob* Barz[1], and *Andreas* Mehner[2]

[1]Fraunhofer Institute for Interfacial Engineering and Biotechnology, Fraunhofer IGB, Nobelstraße 12, 70569 Stuttgart, Germany
[2]Leibniz Institute for Materials Engineering IWT, Badgasteiner Straße 3, 28359 Bremen, Germany

Abstract. Nowadays, it is more important than ever to meet the increasing technical and statutory requirements and to develop new process strategies. In sheet metal forming the low consumption of oil lubrication gets an increasingly important role. The aim in sheet metal forming is to reduce the amounts of lubricants. In the long term, the future sheet metal processing should be able to completely dispense without mineral oil-containing lubricants. Two promising approaches for a dry process design are combined in this paper for the first time and the fundamental feasibility of this new hybrid technology is shown. On the one hand, a novel approach for temporary lubrication of deep-drawing processes with CO_2 as a volatile medium is used. On the other hand, it is supported by the application of an additional hard coating system such as a silicon nitride (Si_3N_4) or tungsten doped a-C:H multilayered (Cr/CrN_x/a-C:H:W/a-C:H) coating system to further reduce tool wear and wear debris of the formed sheets made of DC04 (mat. no.: 1.0338). The results show a low coefficient of friction and reduced wear. Especially for the carbon coating system, there is minor tool wear at a higher surface pressure. By means of the graphite constituent, even a smoothening of the roughness peaks can be recorded. The next step would be the implementation of this hybrid technology on a tool for deep drawing a rectangular cup.

Keywords: Tribology, Lubrication, Dry metal forming

1 Introduction and State of the Art

Tribology is defined as the science of interacting surfaces in relative motion, friction and wear [1]. The system is composed of the three subcomponents (base-) body, counter-body, interfacial element and surrounding medium (environment), see figure 1.

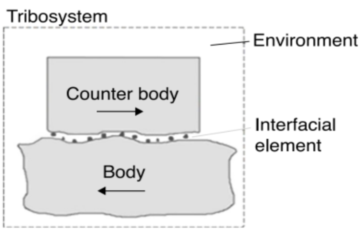

Fig. 1. The Tribosystem provides the basis for the description and analysis of tribological problems [2].

In most forming processes, mineral oil-based lubricants are used as the interfacial medium. The lubricant is able to reduce friction and heat formation in the contact zone, to reduce overall deformation force and energy, and to extend tool life and prevent seizure [3, 4]. Sometimes toxic additives are contained in the lubricant and the formed components have to be cleaned cost intensely and time-consuming for further process steps [5]. Today, there is a great awareness of the environment and its conservation. This inevitably leads to increased requirements and the need for solutions to develop new environmentally friendly tribological systems. Already since the beginning of the 2000s, the legislation in Europe has been changed. Companies are particularly limited in the use of harmful lubricants. In 2007, the EU introduced a new REACH (Registration Evaluation Authorisation and Restriction of Chemicals) law aimed at achieving a high level of protection of human health and the environment from the risk of chemical pollution [6, 7, 8]. Forming of modern high-strength or stainless steels results in a complex tribological system. Reducing the amount of lubricant increases the risk of fretting. In the worst case, it causes a premature tool failure. Nevertheless, attempts are being made to reduce lubricant quantities in order to simultaneously reduce the health and environmental impacts in the manufacturing process [9, 10]. In addition, the use of lubricants subsequent or between two forming operations requires for a complex cleaning process to obtain a clean and oil-free surface. This aspect plays a special role when the components are painted and bonded as a final production [11]. In the past ten years, semi-dry processes and minimum quantity lubrication (MQL) have been implemented in the forming process [12]. The specification of a completely lubricant-free metal forming design could not implement with these strategies. This shows the fact that today still large

* Corresponding author: georg.umlauf@igb.fraunhofer.de

amounts of mineral oil are used for lubrication in the forming process.

Metal forming processes, that completely avoid lubricants, could offer economic and environmental benefits. The definition of dry metal forming does not exclude the use of additives in the process, but focuses on the aspect that no additional purification or drying is required in the subsequent processing step [5]. It is clear that dry metal forming processes present a challenge, since the absence of lubricants typically results in a reduced processing window with respect to the forming limit of the workpiece and its quality. The negative effects of lubricant removal must be compensated with a novel tool concept to ensure a stable and complete forming process.

For this reason, the institutes Fraunhofer IGB and Leibniz-IWT have joined forces for a sub-research project in order to further develop an effective tribosystem for dry forming. In addition to the use of liquid CO_2 as a volatile lubrication a hard material layer is applied on the tool surfaces. The union of these two technologies should result in a new hybrid system with improved wear resistance. The results presented in the following serve first of all as proof in principle. The hybrid system presented here is presented for the first time in this form.

2 Two-way hybrid system

2.1 Lubrication with liquid CO_2

In the priority program (SPP1676) funded by the German Research Foundation (DFG), the institutes IGVP, IFU and IFSW at the University of Stuttgart are working together to develop a manufacturing approach for a mineral oil free forming process. The work explores an environmentally friendly sheet metal forming lubrication system using liquid CO_2 as a lubricant.

The phase diagram of the CO_2 shows, according to figure 2, that CO_2 is in a liquid state at room temperature and a pressure of 57.3 bar. This represents the initial state (red X in figure 2).

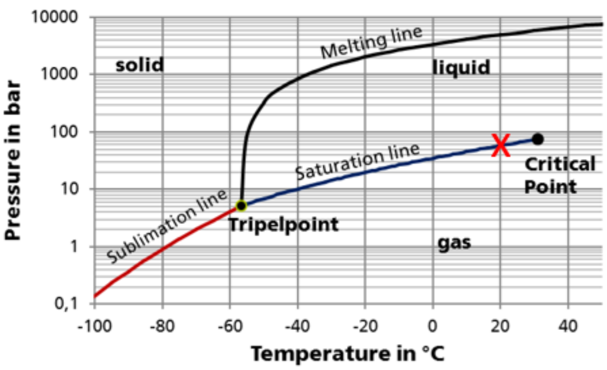

Fig. 2. CO_2 phase diagram, include solid, gas und liqiud phase [13].

Figure 3 shows the overall process sequence of the new CO_2 lubricating system presented here in a simplified form.

First, the liquid lubricant is passed directly into the contact zone and expands there to atmospheric pressure. This causes a cooling and it produces dry ice snow, which acts as a lubricant, achieves a separation of the tool and workpiece, and further reduces the restraining forces.

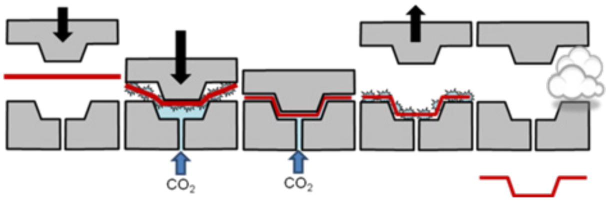

Fig. 3. Process sequence during forming with liquid CO_2 as lubricant replacement [11].

After the forming process, the dry ice is heated by the ambient temperature of the production hall and by the workpiece itself due the deformation induced cohesive frictional heat. So it reverts to the gaseous state of aggregation, as can be seen from the marking in the phase diagram at approximately 1 bar and 23 °C. Thus, there is no oiled component after the forming and further process steps, such as cathodic dip coating or painting, can be carried out without additional purification steps.

2.2 Depostion of a hard coating system

In addition to lubrication with liquid CO_2, a coating of hard material is applied on the active tool surfaces. This subsequent coating should improve the tool life. It may be possible to achieve an additional reduction in friction coefficients when combining a coating with CO_2 compared to a single uncoated CO_2 lubrication. For this purpose, the performance of two different types of hard coatings are tested. The combination of CO_2 lubrication and hard coatings results in the described 2-way hybrid system.

2.2.1 Si_3N_4 coating

Silicon nitride as non-oxide ceramic material has several positive material properties. In addition to the low density (3.44 g/cm^2), it has a very high fracture toughness (6 $MPa*m^{0.5}$) and at the same time good flexural strength (> 800 MPa at 20 °C). Due to the inherent microstructure a high thermal shock resistance is given. These properties make silicon nitride insensitive against thermal shocks and impacts. Si_3N_4 is already used in ball or roller bearings. Also in forming technology Si_3N_4 is used in high stressed tools. The approach for producing this coating will be explained in chapter 3.2.

2.2.2 a-C:H:W/a-C:H PVD coating

The hydrogenated amorphous carbon (a-C:H:W/a-C:H) coating consists of a multi-layered design with a total coatings thickness of about 2.2 µm. As shown in figure 4 b the precise coating design is illustrated. First a thin Cr layer of a few nanometers is deposited acting as soft glue. Then a CrN_x layer is applied with increased hardness of about 8-10 GPa $HIT_{0.01}$ acting as a bonding agent for the upper layers. To further increase the adhesion strength between substrate and functional layers a graded $(Cr,W)C_y$ intermediate layer is introduced. This step also realizes a smooth transition from the metallic into the non-metallic character of the coating. The reason for doping with tungsten of both the graded intermediate and the overlaying a-C:H:W layer (thickness of about 1 µm) is the reducing of the residual coating stresses during the deposition process [14]. This objective is designed to increase the fracture toughness of the whole coating system and to increase the hardness stepwise [15]. Finally, a hard functional a-C:H layer of about 22 GPa $HIT_{0.01}$ is applied for ensuring low dry coefficients of friction of $\mu < 0.2$ and wear against steel and aluminum counter bodies of $k < 3 \cdot 10^{-7} mm^3/Nm$ [16]. In general, a-C:H coatings have a low tendency to adhesion due to the saturation of carbon bonds by hydrogen of the OH groups on the surface [17, 18]. Further details were previously published [19].

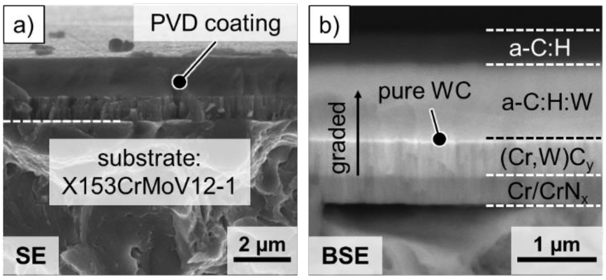

Fig. 4. SEM fracture patterns: a) SE image and b) BSE image at higher magnification of the tested $Cr/CrN_x/(Cr,W)C_y$/a-C:H:W/a-C:H coating system denoted as a-C:H:W/a-C:H [16].

3 Experimental setup

In order to prove the technical fundamental feasibility in a forming process, the exchangeable drawing jaws with laser drilled micro-holes are tested in a strip drawing system. In each experiment CO_2 as volatile lubrication was used. For the new hybrid system, the contact surfaces of the exchangeable tool jaws are additionally applied with different hard coatings. The coating made of Si_3N_4 was carried out at the Fraunhofer-Institute IGB in an ICP plasma reactor. The a-C:H(:W) coating were produced in Bremen at the Leibniz-IWT. For this purpose, an PVD reactive plasma system was used. After the strip drawing tests, a comparison of the determined friction values takes place. Likewise, the roughness values are measured and analyzed.

3.1 Strip drawing test bench

On a strip drawing test system with flat track, it is possible to determine coefficients of friction depending surface pressure per unit area respectively CO_2 flow rate. At the Institute for Forming Technology (IFU, University of Stuttgart), the test bench was modified so that the restraining forces of the CO_2 lubrication system could be measured. For the approach, an experimental tool for supplying the liquid CO_2 directly into the contact zone between tool and sheet was designed and constructed, see figure 5. The strip drawing test bench is described in detail in [20] and [21]. All tests were carried out at room temperature using sheet material DC04 (mat. no.: 1.0338) in rolling direction and repeated three times for statistical reasons.

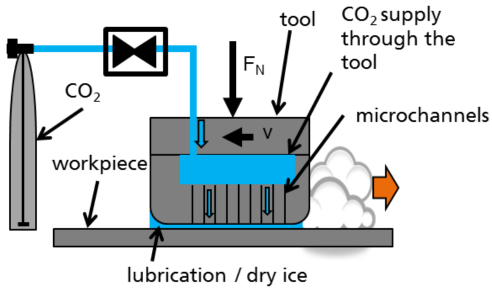

Fig. 5. Schematic illustration of the experimental setup for the operation in the strip drawing test with CO_2 lubrication [11].

In order to apply the liquid CO_2 directly in the effective area between the tool and the workpiece, it must first be passed through the tool. A two-part design of the experimental tool was selected, composed of a hollow body and at 5 mm thin exchangeable jaws made of tool steel X153CrMoV12 (mat. no.: 1.2379). Furthermore, good accessibility for the production of micro-holes is ensured. The construction of the experimental tool can be seen in figure 6. The production of micro-holes is carried out at IFSW, University of Stuttgart and will be explained in more detail in [21].

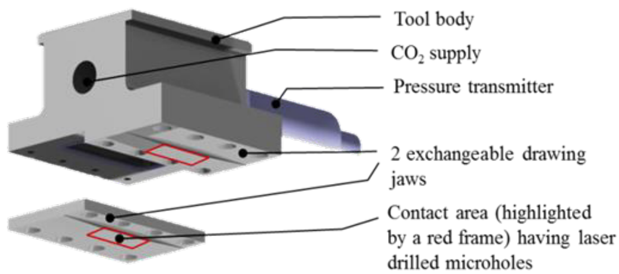

Fig. 6. Modified drawing tool for CO_2 lubrication in strip drawing test [21].

The exchangeable jaws have a contact area of 400 mm^2 in total. Before the exchangeable jaws are used, they are coated with a hard material layer.

3.2 ICP plasma reactor for Si_3N_4 coating

The term ICP-CVD denotes a chemical vapour deposition, system in which an inductively coupled plasma (ICP) source is used. The deposition plasma is ignited via an alternating electromagnetic field within the recipient, which is induced by an inductance coil created by radio frequency (RF). In an ICP reactor, the electrons collide numerous times by the electric field, causing a Joule heating. This is the main mechanism for energy absorption. [22]

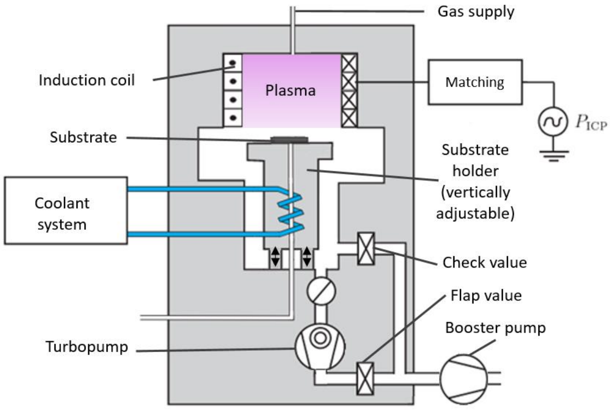

Fig. 7. Simplified illustration of an ICP-PECVD plasma system with the main components, based on [23].

In this work, silicon nitride layers were deposited on the exchangeable jaws by means of the ICP-CVD process and the influence on the frictional behavior in combination with volatile lubricating media was investigated.
The chemical reaction equation for the vapor deposition by ICP-CVD is said to be:

$$3\,SiH_4 + 4\,NH_3 \rightarrow Si_3N_4 + 12\,H_2 \qquad (1)$$

The process duration was 10 minutes with a power input of 2000 W. During the process, the pressure was 0.2 µbar. For optimum oxide-free layer formation, the gas flow was set to 190 cm³/min for SiH_4. The gas mixture ratio was 1:10 (NH_3:SiH_4).

3.3. Reactive magnetron sputtering device for a-C:H:W/a-C:H coating

An industrial reactive magnetron sputtering device from the company CemeCon of the type CC 800/9 SinOx was used for the deposition of the a-C:H:W/a-C:H multilayer coating system. The general principle of the process is illustrated in figure 8. When reactive magnetron sputtering the target material is vaporized due to a momentum exchange caused by ionized process gases. As process gases the noble gases argon and krypton (Ar, Kr) are used. The starting pressure of the device is set to 1 mPa. By applying a negative voltage at the cathodes behind the target materials, released respectively free electrons cause an impact ionization cascade of the noble gases (a). The positive noble gas ions (Ar^+, Kr^+) are accelerated on the target material with high kinetic energy, which initializes the sputtering process of the target atoms (b). Finally, the deposition of the target atoms on the substrate takes place (c). The deposition of the CrN_x layer is realized by the incorporation of pure nitrogen (N_2) as reactive gas. The precursor gas acetylene (C_2H_2) is used for deposition of the a-C:H:W and a-C:H layers. Further details of the deposition process are published in previous publications [16, 19].

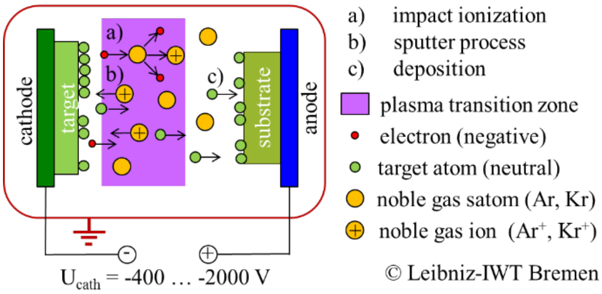

Fig. 8. Simplified illustration of the reactive magnetron sputtering process (source: Leibniz-IWT).

In figure 9 a) the used target configuration is shown in order to apply the mentioned a-C:H:W/a-C:H coating system on a substrate material. The substrate adhesion was determined on a 1.2379 cold working steel, hardened to an overall hardness of about 60±2 HRC (≈800 $HIT_{0.01}$), by Rockwell indentation and scratch tests according to VDI 3198 and DIN EN ISO 1073-3. As illustrated in figure 9 b), the adhesion class HF was 1-2 and the critical load Lc2 was in the range of 30 N [24]. Due to its good adherence no coating failures should be expected due to the modified drawing tool tests.

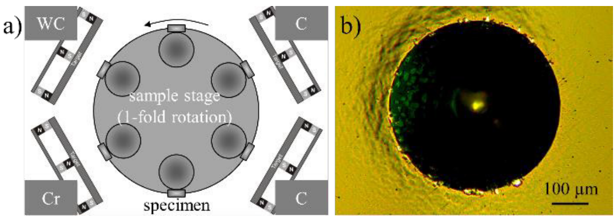

Fig. 9: a) Used target configuration in the CC 800/9 Si_nO_x and b) adhesion strength class (~ HF 1-2) according to VDI 3198.

Figure 10 shows the direct comparison between an exchangeable jaw with an a-C:H:W/a-C:H and a Si_3N_4 coating.

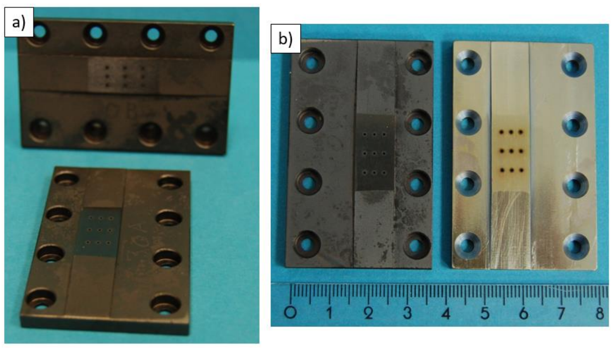

Fig. 10. a) A pair of exchangeable jaws coated with a-C:H:W/a-C:H, b) comparison between a jaw coated with a-C:H:W/a-C:H (left) and Si_3N_4 (right). Both exchangeable jaws are unused.

The next chapter presents the results of the strip drawing tests. Likewise, the roughness was measured after the load and the contact angle with water was determined.

4 Results and Discussion

In this chapter the results of the strip drawing tests are shown and discussed. Figure 11 shows the detailed propagation of the coefficients of friction depending on the applied surface pressure during a volatile CO_2 lubrication in addition with the two used hard coatings. In general, the coefficient of friction increases at higher surface pressures for both applied coatings.

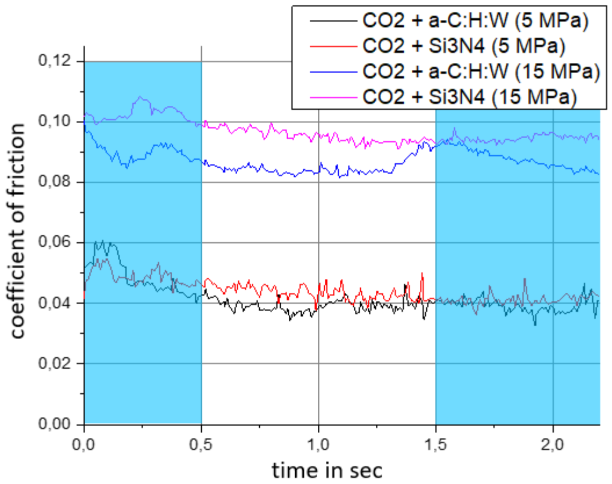

Fig. 11. Detailed coeffenecent of friction for a volatile CO_2 lubrication in addition with two hard coatings at two different surface pressures.

For an averaged coefficient of friction, not the entire drawing distance is considered, otherwise the running-in behavior would change this value too much. Only the recorded values of 0.5 to 1.5 sec are included in the determination. This results in a friction coefficient of 0.039 for the Si_3N_4 coating at a surface pressure of 5 MPa. For comparison, the friction coefficients for exchangeable jaws without hard material coating are plotted in figure 12.

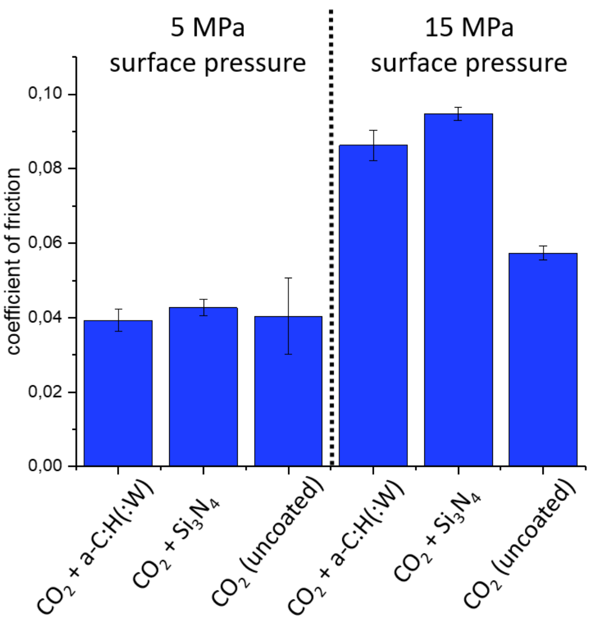

Fig. 12. Representation of the coefficients of friction for coated and uncoated exchangeable jaws in combination with a volatile CO_2 lubrication, each with 5 and 15 MPa surface pressure.

For a surface pressure of 5 MPa, all three exchangeable jaws are at the same low level. Only at a surface pressure of 15 MPa, the coated exchangeable jaws have a higher coefficient of friction compared to the uncoated (just CO2 lubrication). This can be attributed to excessive wear of the surface around the micro-hole (see figure 13). So there was no smooth flat surface on the entire contact area.

However, these results are only partially comparable, since the uncoated replaceable plates have been previously hardened and thus more resistant.

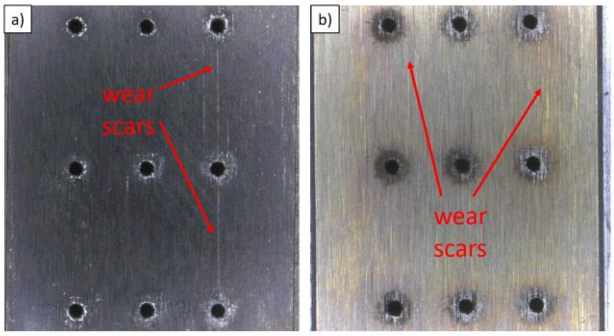

Fig. 13. Wear scars and wear around the mirco-holes at the a-C:H:W/a-C:H coating system (a) and Si_3N_4 coating (b) after strip drawing test.

Figure 13 shows the wear patterns of the applied hard coatings. It can be observed that coating failure took place especially around the mirco-holes. Previous quality investigations of uncoated exchangeable jaws around the mirco-holes at the outlet showed a bulge (see figure 14). This is up to 0.025 mm. This increase significantly influences the coefficient of friction and explains the abrasion of the hard material layers around the mirco-holes. The current object of the investigations at IFSW is to produce the mirco-holes without a material bulge.

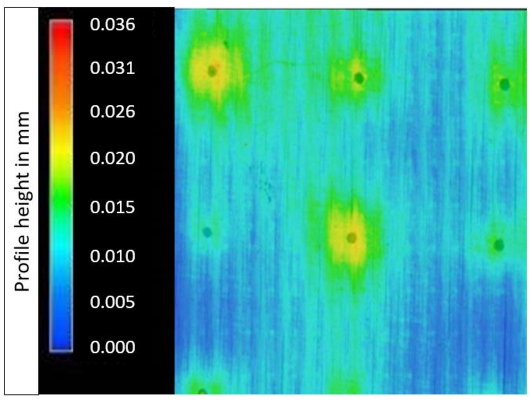

Fig. 14. Microscope images with height profile of the exchangeable drawing jaws show an significant increase around the mirco-holes of up to 0.025 mm (source : IFU; University Stuttgart).

However, additional line-shaped wear scars are found mainly located between the drill holes in drawing direction of the tools. Further verification measurements were carried out on a profilometer determining the roughness profiles and the resulting surface roughness R_a. In addition, measurements of the contact angle were performed to identify the wetting behavior.

The results of the roughness measurements were determined by four single lines whereas each line has a length of about 5 mm at the contact area (perpendicular to the drawing direction). Figure 16 shows representative roughness profile lines measured at the a-C:H:W/a-C:H coating system (a) respectively at the Si_3N_4 coating (b).

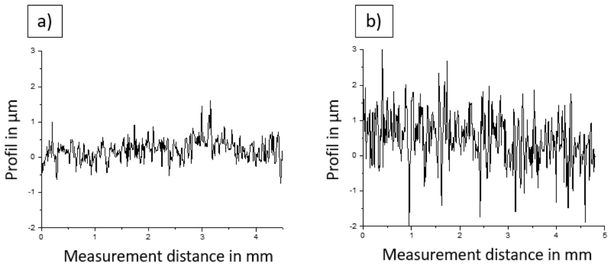

Fig. 15. Roughness R_a after a strip drawing test for a) a-C:H:W/a-C:H coating and b) Si_3N_4 coating.

The mean roughness value for a-C:H:W/a-C:H coating system R_a is between 0.19 and 0.21 µm (Si_3N_4 coating: R_a is between 0.52 to 0.57 µm; 3 measurements per line) after the strip drawing test. The water contact angles before and after the strip drawing test were measured in order to get conclusions about the wear and roughening.
At the a-C:H:W/a-C:H coating system the water contact angle drops from 74.98 ± 1.23° to 53.13 ± 2.03° degrees. Whereas with a Si_3N_4 coating, the contact angle of water increases from 52.68 ± 0.96° to 84.47 ± 3,13°. The decrease in an a-C:H:W/a-C:H coating indicates a leveling and shifting of the applied graphite coatings. In contrast, the Si_3N_4 coating must have been roughened, as the surface becomes more hydrophobic. This effect can be attributed to the so-called Cassie-Baxter case. [25] This means that the surface is finely structured and it increases the water contact angle. In this special case, a surface micro-structuring (uniform or irregular) is not desired because it also increases the coefficient of friction.

5 Conclusion

Previous researches has shown that a deep drawing process of a U-profile [21] as well as for a rectangular cup [26] with pure CO_2 as a volatile lubrication without mineral-oil are possible. With an additional coating, no further reduction in the coefficient of friction compared to pure CO_2 lubrication with uncoated tools in a strip drawing test bench was achieved. Especially at 15 MPa surface pressure, the coefficient of friction increases with regard to the uncoated reference. However, a roughening effect takes place especially at the Si_3N_4 coating. This leads to increased wear and subsequently to higher coefficients of friction. However, another important observation is that at both applied coatings the layers are completely or partially worn around the drill holes (compare to figure 13). Despite the additional CO_2 lubrication, this could be an indication that there is no complete surface separation of the DC04 sheet metal and the coated exchangeable tool jaws. Solid state contact around the drill holes would be the consequence which explains the observed wear patterns. Formed wear debris, e. g. removed coating or tool material, at the mirco-holes is ploughed through the coating in strip drawing direction which could be an adequate explanation of the observed wear patterns in figure 13. For this reason, further wear analyzes have to be carried out at the mirco-holes and between by scanning electron microscopy (SEM) and energy dispersive X-ray spectroscopy (EDS) in order to finally clarify the reasons of this wear pattern. Next to that, the quality of flatness of the jaws surfaces in the area of the drill holes has to be quantified by laser confocal microscopy to ensure solid body separation during strip drawing. Also the fine structure of the wear scars have to be measured to derive a link of the dimension of ploughed wear debris. Related to the wear analyzes it should be possible to derive sufficient strategies with regard to the coating development. It needs to be clarified, whether an insufficient coating adhesion strength to the substrate material, a too low coating fatigue resistance or failures of the tool material due to the laser drilling process itself are responsible for such premature wear patterns.

The hybrid approach for dry lubrication with a primary CO_2 lubrication and additional hard material coating, which is presented for the first time in this paper, is initially used exclusively for basic investigations. Further investigations must be carried out for a final evaluation. It can be concluded:
The coatings presented in this purpose could a promising approach. The layer durability must be improved. In addition, the laser drilling process must be material compatibility so that there is no material bulge around the borehole. With regard to initial endurance tests at the IFU, an additional plasma technological layer should be applied to the hardened deep drawing tool.

The financial support of this study by the German Research Foundation (DFG) within the framework of the priority programme *Sustainable Production through Dry Processing in Metal Forming* (SPP 1676) is gratefully acknowledged. The authors thank Christoph Wörz from the Institute for Metal Forming Technology for provision of strip drawing test bench. Thanks also to Andreas Schulz from the Institute of Interfacial Process Engineering and Plasma Technology for assistance in measuring with the profilometer.

References

[1] Gesellschaft für Tribologie (Hrsg.): Tribologie – Verschleiß, Reibung, Definitionen, Begriffe, Prüfung. GfT-Arbeitsblatt 7, Aachen, (2002)
[2] Zum Gahr K.-H. : Microstructure and wear of materials. Tribology series, 10. New York: Elsevier, (1987)
[3] P. Skakun, I. Kacmarcik, T. Pepelnjak, O. Luzanin, A. Inavisevic, M. Milutinovic: Compersion of conventional and new lubricants for cold forming. 34th International conference on production engineering, (2011)
[4] M. Arentoft, N. Bay, P.T. Tang, J.D. Jensen: A new lubricant carrier for metal forming. CIRP Annals - Manufacturing Technology 58,243–246 (2009)
[5] F. Vollertsen, F. Schmidt: Dry Metal Forming: Definition, Chances and Challenges. Int. J. Precision

Engineering and Manufacturing – Green Technology 1/1, 59-62 (2014)
[6] N. Bay, A. Azushima, P. Groche, I. Ishibashi, M. Merklein, M. Morishita, T. Nakamura, S. Schmid, M. Yoshida: Environmentally benign tribo-systems for metal forming. CIRP Annals - Manufacturing Technology 59, 760–780 (2010)
[7] European Parliament, Council REACH, EC Regulation No. 1907/2006 of the European Parliament and of the Council, (2006)
[8] ICFG Doc. 10/95: Lubrication Aspects in Cold Forging of Aluminium and Aluminium Alloys. The International Cold Forging Group. WIRE 1, 1–12 (1996)
[9] Institute of Health and Consumer Protection (IHCP): European Union Risk Assessment Report, alkanes, C10-13, chloro (CAS No. 85535-84-8), (2008)
[10] A. Mousavi, A. Brosius: Track Tool concepts for dry forming. Dry Met. Forming OAJ FMT 1, 79–82 (2015)
[11] M. Liewald, T. Graf, T. Hirth, M. Singer, A. Feuer, E. Zahedi, G. Umlauf : Tribosysteme für die Kaltumformung auf der Basis von flüchtigen Schmiermedien und laserstrukturierten Oberflächen. Dry Met. Forming OAJ FMT 1, 22-33 (2015)
[12] P. C. Priarone, M. Robiglio, L. Settineri, V. Tabeldo: Milling and turning of titanium aluminides by using minimum quantity lubrication. New Production Technologies in Aerospace Industry - 5th Machining Innovations Conference, Procedia CIRP 24, 62 – 67 (2014)
[13] ChemicaLogic Corporation, http://www.chemicalogic.com/Pages/default.aspx (2015)
[14] X. Chen, Z. Peng, Z. Fu, S. Wu, W. Yue, C. Wang: Microstructural, mechanical and tribological properties of tungsten-gradually doped diamond-like carbon films with functionally graded interlayers. Surface and Coatings Technology, Vol. 205, 3631-3638 (2011)
[15] A. Czyzniewski: Optimising deposition parameters of W-DLC coatings for tool materials of high speed steel and cemented carbide. Vacuum, Vol. 66, 2140-2147 (2012)
[16] H. Hasselbruch, M. Herrmann, A. Mehner, H.-W. Zoch, B. Kuhfuss: Development, characterization and testing of tungsten doped DLC coatings for dry rotary swaging. MATEC Web of Conference, Vol. 21, 1-7 (2015)
[17] M. Murakawa, M. Jin, M. Hyashi: Study on semidry/dry wire drawing using DLC coated dies. Surface and Coatings Technology, Vol. 177-178, 631-637 (2014)
[18] H. Hetzner: Systematische Entwicklung amorpher Kohlenstoffschichten unter Berücksichtigung der Anfoderungen der Blechmassivumformung. Dissertation, University of Erlangen, (2014)
[19] H. Hasselbruch, M. Herrmann, A. Mehner, B. Kuhfuss, H.-W. Zoch: Incremental dry forging – Interaction of W-DLC coatings and surface structures for rotary swaging tools. Proceedia Manufacturing, Vol. 8, 541-548 (2017)
[20] M. Liewald, S. Wagner, D. Becker: Ausstattung und Kompetenzen des Tribologie-Labors am Institut für Umformtechnik der Universität Stuttgart. IDDRG-Sitzung Düsseldorf, (2005)
[21] C. Wörz, E. Zahedi, G. Umlauf, M. Liewald, R. Weber, T. Graf, G. Tovar: Tiefziehen eines U-Profils mit flüchtigen Medien als Schmierstoffersatz. Dry Met. Forming OAJ FMT 3, 50-61 (2017)
[22] T. Okumura: Inductively Coupled Plasma Sources and Applications, Hindawi Publishing Corporation Physics Research International, Vol. 2010, (2010)
[23] S. M. Jatta, Plasmaunterstütze Abscheidung von dielektischen Schichten zur Entwicklung von mikromechanisch abstimmbaren optischen Komponenten. Dissertation, TU Darmstadt, (2010)
[24] H. Hasselbruch, A. Mehner, H.-W. Zoch: Influence of plasma nitriding parameters and subsequent surface finishing on the adhesion strength of tungsten doped PVD a-C:H coatings. Proceedings of the 13th International Conference of THE"A" Coatings, Greece, 169-179 (2017)
[25] W. M. Sigmund, SH. Hsu: Cassie-Baxter Model. in Encyclopedia of Membranes, Springer, Berlin, (2016)
[26] C. Wörz, G. Reichardt, M. Liewald, E. Zahedi, R. Weber, T. Graf : Dry deep drawing of a rectangular cup assisted by volatile media injected from laser-drilles mircoholes. Dry Met. Forming OAJ FMT 5, (2018)